

Gravitational time delay effects by Kerr and Kerr-Newman black holes in strong field limits

Tien Hsieh, Da-Shin Lee,* and Chi-Yong Lin†

Department of Physics, National Dong Hwa University,

Hualien 97401, Taiwan, Republic of China

(Dated: November 8, 2021)

Abstract

We study the time delay between two relativistic images due to strong gravitational lensing of the light rays caused by the Kerr and Kerr-Newman black holes. Using the known form of the deflection angle in the strong deflection limit (SDL) allows us to analytically develop the formalism for the travel time of the light from the distant source winding around the black hole several times and reaching the observer. We find that the black hole with higher mass or with spin of the extreme black hole potentially have higher time delay. The effect of the charge of the black hole enhances the time delay between the images lying on the opposite side of the optical axis resulting from the light rays when one light ray is in the direct orbit and the other is in the retrograde orbit. In contrary, when both light rays travel along either direct or retrograde orbits giving the images on the same side of the optical axis, the charge effect reduces the time delay between them. We then examine the time delay observations due to the galactic and supermassive black holes respectively.

PACS numbers: 04.70.-s, 04.70.Bw, 04.80.Cc

*Electronic address: dslee@gms.ndhu.edu.tw

†Electronic address: lcyong@gms.ndhu.edu.tw

I. INTRODUCTION

The gravitational deflection of light provides one of the first observational tests of General Relativity (GR) [1–4]. Under a weak-field approximation gravitational lenses have been investigated with intensity to successfully explain various lensing phenomena in a broad array of astrophysical contexts, ranging from stars through galaxies and clusters of galaxies up to the large scale structure of the universe [5, 6]. When the lens is a very compact object (e.g. a black hole), one must go beyond the weak field approximation. There have been significant theoretical efforts over several decades for understanding lensing from strong field perspectives [7–16]. Inspired by the first image of the black hole captured by the Event Horizon Telescope [17–19], gravitational lensing will also become an important measures to explore the properties of the isolated dim black hole.

The gravitational lens equation that is suited to study large deflection of light rays was developed by Virbhadra and Ellis with an application to the Schwarzschild black hole [7]. Later, the definition of an exact lens equation without reference to the background spacetime was proposed by Frittelli *et al.*, where they constructed the exact lens equation explicitly in the Schwarzschild spacetime [8]. As for the general spherically symmetric and static spacetime, the strong field limit was first studied analytically by Bozza [9–11] and later by Tsukamoto [15, 16], showing that the deflection angle $\hat{\alpha}(b)$ of light rays in the limit of $b \rightarrow b_c$ can be approximated in the following simple form,

$$\hat{\alpha}(b) \approx -\bar{a} \log \left(\frac{b}{b_c} - 1 \right) + \bar{b} + O(b - b_c) \log(b - b_c) \quad (1)$$

with the two parameters \bar{a} and \bar{b} given in terms of black hole's parameters. In [20], we extended the works of [10, 15] and find the analytic form of \bar{a} and \bar{b} for Kerr and Kerr-Newman black holes, respectively, with the analytical closed-form expressions of the deflection angles obtained in [21] and [22]. In [20], we have examined the lensing effects due to the black hole when the light rays from the source circle around the black hole multiple times in the strong deflection limit (SDL) along a direct orbit (red line) or a retrograde orbit (blue line), giving two sets of the relativistic images as illustrated in Fig.(1). In [23, 24], some relations between gravitational lensing in the SDL and the frequencies of the quasinormal modes of black holes are found, where the coefficients \bar{a} and \bar{b} can give an alternative method for the measurement of quasinormal frequencies of the black holes, which play importance roles in

gravitational-wave astrophysics.

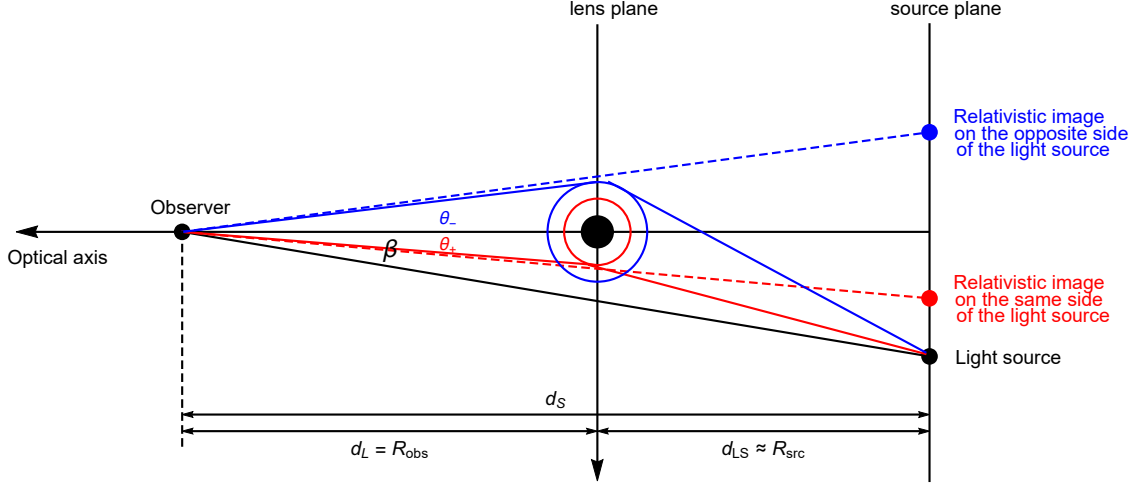


FIG. 1: Gravitational lens about relativistic images. Considering the Kerr or the Kerr-Newman black hole with angular momentum of the clockwise rotation, the light rays are emitted from the source, and circle around the black hole multiple times in the SDL along a direct orbit (red line) or a retrograde orbit (blue line). The graph illustrates two sets of the relativistic images.

In strong gravitational lensing phenomena, the apparent angles of the images and the time delay between relativistic images are the most important observable that can be widely used to reveal information about the lens from the resulting effects of the light rays [25–30]. According to [25], Bozza developed the following formula of the travel time of the light

$$T(b) = -2\tilde{a} \log \left(\frac{b}{b_c} - 1 \right) + \tilde{b}(R_{src}) + \tilde{b}(R_{obs}) + \mathcal{O}((b - b_c) \log(b - b_c)) \quad (2)$$

in the strong field limit by introducing another two parameters \tilde{a} and \tilde{b} . In (2), \tilde{a} just depends on the black hole's parameters whereas \tilde{b} not only depends on the black hole's parameters but also has the dependence of the distance of the source R_{src} and the observer R_{obs} from the lens. Following [25], we will work on the time delay effects due to the Kerr and Kerr-Newman black holes [32–34], the two important solutions resulting from the Einstein equations plus the Maxwell equations to incorporate the charge of the black hole [2, 31]. In this work, we will explicitly find out the analytical expressions of the coefficients \tilde{a} and \tilde{b} with which to extract interesting features of the time delay observations.

Layout of the paper is as follows. In Sec.II, we first develop the formalism of the travel

time of the light from the source circulating around the black hole and reaching the observer. Then we derive the analytic form of \tilde{a} and \tilde{b} in⁴ (2) for the cases of Kerr and Kerr-Newman black holes, respectively, and check the consistency with the known results from taking the proper limits of the black holes's parameters. In addition, we will find their approximate expressions in the limits as the spin of the black hole is small $a \rightarrow 0$, as well as the spin reaches the extreme value $a \rightarrow M$ ($a \rightarrow \sqrt{M^2 - Q^2}$) of the extreme Kerr (Kerr-Newman) black holes. In Sec. III, the analytical expressions of \tilde{a} and \tilde{b} are then applied to compute the time delay between relativistic images obtaining their general features. The approximately analytical forms of \tilde{a} and \tilde{b} are very useful to interpret the time delay behavior in the appropriate limits. The effects of angular momentum and charge of the black holes to the time delay observations will be summarized in the closing section. Additionally, the closed-form expression of the deflection angle due to the Kerr and/or the Kerr-Newman black holes is summarized in Appendix A. In particular, we present the results of the radius of the innermost circular motion of light rays as well as the associated critical impact parameters as a function of the black hole's parameters. These will serve as the important inputs to find the values of the coefficients \bar{a} and \bar{b} in the SDL deflection angle. In Appendix B, we provide useful integral formulas to find the coefficients \tilde{a} and \tilde{b} . In this paper, we have used $c = G = 1$ units, unless otherwise specified.

II. TIME DELAY DUE TO BLACK HOLES IN THE STRONG FIELD LIMIT

We consider nonspherically symmetric spacetimes of the Kerr and Kerr-Newman metrics to obtain the travel time $T(b)$ of light from the source to the observer for a given impact parameter b . In the SDL, as $b \rightarrow b_c$, $T(b)$ can be approximated in the form (23) with two parameters \tilde{a} and \tilde{b} as a function of the black hole's parameters and the distances of the source and the observer from the black hole. In what follows, we will discuss these two kinds of the black holes separately.

A. Kerr black holes

The spacetime outside of the horizon of the Kerr black hole with the gravitational mass M and angular momentum per unit mass $a = J/M$ is described by the line element below

$$\begin{aligned} ds^2 &= g_{\mu\nu}dx^\mu dx^\nu \\ &= -\frac{(\Delta - a^2 \sin^2 \theta)}{\Sigma} dt^2 - \frac{a \sin^2 \theta (2Mr)}{\Sigma} (dt d\phi + d\phi dt) \\ &\quad + \frac{\Sigma}{\Delta} dr^2 + \Sigma d\theta^2 + \frac{\sin^2 \theta}{\Sigma} ((r^2 + a^2)^2 - a^2 \Delta \sin^2 \theta) d\phi^2 \end{aligned} \quad (3)$$

with

$$\Sigma = r^2 + a^2 \cos^2 \theta, \quad \Delta = r^2 + a^2 - 2Mr. \quad (4)$$

The outer (inner) event horizon r_+ (r_-) can be found by solving $\Delta(r) = 0$, given by

$$r_\pm = M \pm \sqrt{M^2 - a^2} \quad (5)$$

with the condition $M^2 > a^2$. Notice that although the inner event horizon r_- is introduced, here we consider the light rays traveling outside the outer horizon. Due to the fact that the metric component functions are independent on t and ϕ , and thus the metric itself is both stationary and axial-symmetric. Together with 4-velocity of light defined in terms of the affine parameter, the conserved quantities of light ray's energy and azimuthal angular momentum along a geodesic obeying $u^\mu u_\mu = 0$ can be obtained from the Killing vectors $\varepsilon \equiv -\xi_{(t)}^\mu u_\mu$ and $\ell \equiv \xi_\phi^\mu u_\mu$, where the associated Killing vectors $\xi_{(t)}^\mu$ and $\xi_{(\phi)}^\mu$ are $\xi_{(t)}^\mu = \delta_t^\mu, \xi_\phi^\mu = \delta_\phi^\mu$. The light can be traversing along the direction of the black hole rotation or opposite to it with the impact parameter defined as

$$b_s = s \left| \frac{\ell}{\varepsilon} \right| \equiv s b, \quad (6)$$

where $s = \text{Sign}(\ell/\varepsilon)$ and b is the positive magnitude. The parameter $s = +1$ for $b_s > 0$ will be referred to as direct orbits, and those with $s = -1$ for $b_s < 0$ as retrograde orbits (see Fig.(1) for the sign convention). In this paper, the light rays are restricted to traveling on the equatorial plane of the black hole, where $\theta = \pi/2$, and $\dot{\theta} = 0$. In the end, their dynamics can be summarized into the equation of motion along the radial direction in the form [22]

$$\frac{1}{b^2} = \frac{\dot{r}^2}{\ell^2} + W_{\text{eff}}(r), \quad (7)$$

from which to define the effective potential function W_{eff} as

$$W_{\text{eff}}(r) = \frac{1}{r^2} \left[1 - \frac{a^2}{b^2} - \frac{2M}{r} \left(1 - \frac{a}{b_s} \right)^2 \right]. \quad (8)$$

We consider that a light ray starting in the asymptotic region approaches the black hole, and then turns back to the asymptotic region reaching the observer. During the journey, the turning point, the closest approach distance to a black hole r_0 , crucially depends on the impact parameter b , determined by

$$\frac{\dot{r}^2}{\ell^2} \Big|_{r=r_0} = \frac{1}{b^2} - W_{\text{eff}}(r_0) = 0. \quad (9)$$

The smallest radius r_{sc} of the innermost trajectories of light of relevance to the apparent shape of the black hole is given by the turning point r_0 located at the maximum of $W_{\text{eff}}(r)$ with the critical impact parameter b_{sc} obeying the equation [22]

$$\frac{dW_{\text{eff}}(r)}{dr} \Big|_{r=r_{sc}} = 0. \quad (10)$$

The solutions are reviewed in Appendix A. In fact, the values of b_{sc} and r_{sc} are the key inputs to determine the features of the deflection angle of the distant light sources due to the strong gravitational lensing effects. Given the effective potential W_{eff} in (8), the nonzero spin of the black holes induces more repulsive effects to the light in the direct orbits than those in the retrograde orbits due to the $1/r^3$ term. Near horizon the repulsive effects turn out effectively to prevent the light in the direct orbits from collapsing into the event horizon. As a result, this shifts the innermost circular trajectories of the light rays toward the black hole with the smaller critical impact parameter b_{+c} than b_{-c} in the retrograde orbits as shown in [21, 22]. As such, when a increases, the impact parameter b_{+c} decreases whereas b_{-c} increases instead. In addition, the previous work also shows that the deflection angle $\hat{\alpha}(b)$ of light for a given impact parameter b , which in the SDL as $b \rightarrow b_c$, can be approximated in the form

$$\hat{\alpha}(b) \approx -\bar{a} \log \left(\frac{b}{b_c} - 1 \right) + \bar{b} + O(b - b_c) \log(b - b_c), \quad (11)$$

where the two parameters \bar{a} and \bar{b} are obtained in terms of black hole's parameters (See brief review in Appendix A).

Now consider the travel time of the light from the source to the observer, which pass by the black hole with the closest approach distance r_0 as

$$T(r_0) = \int_{R_{src}}^{r_0} \left| \frac{dt}{dr} \right| dr + \int_{r_0}^{R_{obs}} \left| \frac{dt}{dr} \right| dr. \quad (12)$$

The parameters R_{src} and R_{obs} are the distance between the black hole and the source or observer, respectively. Following [22], we can rewrite the equation of motion dt/dr in (9) by introducing a new variable z defined by $z = 1 - r_0/r$ as

$$\frac{dt}{dz} = \frac{r_0}{(1-z)^2} \frac{-a \frac{2M}{r_0} (1 - \frac{a}{b})(1-z)^3 + \frac{r_0^2}{b} + \frac{a^2}{b}(1-z)^2}{1 - \frac{2M}{r_0}(1-z) + \frac{a^2}{r_0^2}(1-z)^2} \frac{1}{\sqrt{B(z, r_0)}}, \quad (13)$$

where the function $B(z, r_0)$ has the trinomial form in z

$$B(z, r_0) = c_1(r_0)z + c_2(r_0)z^2 + c_3(r_0)z^3 \quad (14)$$

with the coefficients

$$c_1(r_0) = -6Mr_0 \left(1 - \frac{a}{b_s}\right)^2 + 2r_0^2 \left(1 - \frac{a^2}{b^2}\right), \quad (15)$$

$$c_2(r_0) = 6Mr_0 \left(1 - \frac{a}{b_s}\right)^2 - r_0^2 \left(1 - \frac{a^2}{b^2}\right), \quad (16)$$

$$c_3(r_0) = -2Mr_0 \left(1 - \frac{a}{b_s}\right)^2. \quad (17)$$

Then, R_{src} and R_{obs} can be expressed by z as, $Z_{src} = 1 - r_0/R_{src}$ and $Z_{obs} = 1 - r_0/R_{obs}$, respectively. The observer and the source are supposedly very far from the black holes, $R_{src}, R_{obs} \gg r_0$, then both $Z_{src}, Z_{obs} \rightarrow 1$.

We rewrite part of the integrand in (13) by the partial fraction,

$$\begin{aligned} & \frac{1}{(1-z)^2} \frac{-a \frac{2M}{r_0} (1 - \frac{a}{b})(1-z)^3 + \frac{r_0^2}{b} + \frac{a^2}{b}(1-z)^2}{1 - \frac{2M}{r_0}(1-z) + \frac{a^2}{r_0^2}(1-z)^2} \\ &= \frac{r_0^2}{a^2 b} \frac{1}{\left[\frac{\tilde{C}_-}{z - z_-} + \frac{\tilde{C}_+}{z - z_+} + \frac{r_0^2}{(1-z)^2(z - z_-)(z - z_+)} \right]} \end{aligned} \quad (18)$$

The roots and the corresponding coefficients \tilde{C}_- , \tilde{C}_+ in the Kerr case are

$$z_- = 1 - \frac{r_0 r_-}{a^2}, \quad (19)$$

$$z_+ = 1 - \frac{r_0 r_+}{a^2}, \quad (20)$$

$$\tilde{C}_- = \frac{-2Mabr_- + a^4 + 2Ma^2r_-}{2r_0\sqrt{M^2 - a^2}}, \quad (21)$$

$$\tilde{C}_+ = \frac{2Mabr_+ - a^4 - 2Ma^2r_+}{2r_0\sqrt{M^2 - a^2}}, \quad (22)$$

with r_+ (r_-) being the outer (inner) horizon of a Kerr black hole defined in (5). Notice that $z_-, z_+ \leq 0$, for all spin a .

Then the travel time of the light can be calculated as a function of the closest approach distance r_0 from (13) giving

$$T(r_0) = I(Z_{src}, r_0) + I(Z_{obs}, r_0), \quad I(Z, r_0) = \int_0^Z f(z, r_0) dz. \quad (23)$$

In the SDL, when $r_0 \rightarrow r_{sc}$, $c_1(r_0) \rightarrow 0$ in (15) obtained from (10), the integral $f(z, r_0) \rightarrow 1/z$ for small z will lead to the logarithmic divergence as $r_0 \rightarrow r_{sc}$. Let us now define a new function $f_D(z, r_0)$

$$f_D(z, r_0) = \frac{r_0^3}{a^2 b} \left[\frac{\tilde{C}_-}{z - z_-} + \frac{\tilde{C}_+}{z - z_+} + \frac{r_0^2}{(1 - z)^2 (z - z_-)(z - z_+)} \right] \frac{1}{\sqrt{c_1(r_0)z + c_2(r_0)z^2}}, \quad (24)$$

and also $f_R(z, r_0) = f(z, r_0) - f_D(z, r_0)$. The integral of f_R over z is thus finite given by (112) in Appendix B and contributes part of \tilde{b} in (2), denoted by \tilde{b}_R . The divergent part due to an integral of the function $f_D(z, r_0)$ over z can be obtained from the result of (111), giving not only to \tilde{a} for the logarithmic divergence but also contributing partly to the formula of \tilde{b} for the regular part in (2), denoted by \tilde{b}_D . The possible divergence means that the light rays spend long time in circling around the black hole as the impact parameter is near its critical value, $b \rightarrow b_{sc}$. Notice that in the SDL, all the coefficients c_1, c_2 and c_3 in (15)-(17) will be evaluated at $r_0 = r_{sc}$. However, since $c_1(r_{sc}) \equiv c_{1sc} = 0$, we need the expansion of the coefficient $c_1(r_0)$ given by (15) to the next order, namely

$$c_1(r_0) = c'_{1sc}(r_0 - r_{sc}) + \mathcal{O}(r_0 - r_{sc})^2. \quad (25)$$

The subscript “ sc ” denotes evaluating the function at $r = r_{sc}$. The prime means the derivative with respect to r_0 . Using $c_{1sc} = 0$ in (15) leads to

$$c_{3sc} = -\frac{2}{3}c_{2sc}. \quad (26)$$

Furthermore, one can write $c_1(r_0)$ in terms of $b - b_{sc}$. To achieve it, the expansion of the impact parameter $b(r_0)$ at r_{sc} reads

$$b(r_0) = b_{sc} + \frac{b''_{sc}}{2!}(r_0 - r_{sc})^2 + \mathcal{O}(r_0 - r_{sc})^3. \quad (27)$$

Combining (25) and (27) gives

$$\lim_{r_0 \rightarrow r_{sc}} c_1(r_0) = \lim_{b \rightarrow b_{sc}} c'_{1sc} \sqrt{\frac{2b_{sc}}{b''_{sc}}} \left(\frac{b}{b_{sc}} - 1 \right)^{1/2}. \quad (28)$$

Thus, the straightforward calculations give the coefficients \tilde{a} and $\tilde{b} = \tilde{b}_R + \tilde{b}_D$ in the key formula (2) as

$$\tilde{a} = \frac{r_{sc}^3}{2b_{sc}\sqrt{c_{2sc}}} \left[\frac{2M + r_{sc}}{2r_{sc}} + \frac{\tilde{C}_{-sc}}{r_{sc}r_- - a^2} + \frac{a^6}{r_-^2(r_{sc}r_- - a^2)r_{sc}(r_+ - r_-)} \right] + (- \leftrightarrow +) , \quad (29)$$

$$\begin{aligned} \tilde{b} = & \frac{1}{2}\tilde{a} \log \left(\frac{8c_{2sc}^2 Z^2 b''_{sc}}{c_{1sc}^2 b_{sc}} \right) \\ & + \frac{r_{sc}^3}{2b_{sc}\sqrt{c_{2sc}}} \left[\frac{\sqrt{3}\sqrt{3-2Z}}{1-Z} + 2\sqrt{3}\frac{M}{r_{sc}} \log \left(\frac{2-Z+\sqrt{3-2Z}}{2+\sqrt{3}} \frac{1}{1-Z} \right) \right. \\ & \quad \left. - 3 - \frac{r_{sc}^2}{(a^2 - 2Mr_{sc} + r_{sc}^2)} \log \tilde{N}(Z, a) \right] \\ & + \frac{r_{sc}^3 \tilde{C}_-}{b_{sc}\sqrt{c_{2sc}}(a^2 - r_{sc}r_-)} \left[\log \tilde{N}(Z, a) - \frac{\sqrt{3}a}{\sqrt{a^2 + 2r_{sc}r_-}} \log \tilde{M}(Z, a, r_-) \right] \\ & - \frac{r_{sc}^2}{b_{sc}\sqrt{c_{2sc}}} \frac{\sqrt{3}a^7}{r_-^2(a^2 - r_{sc}r_-)\sqrt{a^2 + 2r_{sc}r_-}(r_+ - r_-)} \log \tilde{M}(Z, a, r_-) + (- \leftrightarrow +) , \end{aligned} \quad (30)$$

where

$$\tilde{M}(Z, a, r_\pm) = \frac{a^2 - r_{sc}r_-}{a^2 - r_{sc}r_- - Za^2} \frac{(2-Z)a^2 + r_{sc}r_\pm + a\sqrt{3-2Z}\sqrt{a^2 + 2r_{sc}r_\pm}}{2a^2 + r_{sc}r_- + a\sqrt{3}\sqrt{a^2 + 2r_{sc}r_\pm}} , \quad (31)$$

$$\tilde{N}(Z, a) = \frac{3 - Z + \sqrt{3}\sqrt{3-2Z}}{6} . \quad (32)$$

This is one of the main results in this paper. The analytical expressions of \tilde{a} and \tilde{b} in the SDL travel time of the light around the black hole can be applied to compute the time delay between two relativistic images. Through comparing with observations can provide information on the black hole's parameters [25].

Now let us compare with the some known results on the Schwarzschild black holes in [25]. In the limit of $a \rightarrow 0$, $r_+ \rightarrow 2M$, $r_- \rightarrow a^2/2M$, $\tilde{C}_{+c} \rightarrow a$, $\tilde{C}_{-c} \rightarrow a^3$, and $c_2 \rightarrow r_c^2$ using $c_{1sc} = 0$. Since $b''_c \rightarrow \sqrt{3}/M$ and $r_c = 3M$, the coefficient \tilde{a} in (29) can be simplified to

$$\tilde{a} = \frac{3\sqrt{3}}{2}M. \quad (33)$$

Together with $\bar{a} = 1$ in the expression of the SDL deflection angle in (11) gives the expected relation

$$\frac{2\tilde{a}}{\bar{a}} = b_c \quad (34)$$

for the spherically symmetric black holes. It is worthwhile to mention that the relation (34) still holds true in the Kerr black holes with nonspherically symmetric metric. One can verify this result easily from substituting the equations of the light sphere r_{sc} in (89) and the critical impact parameter b_{sc} in (91) into the ratio of \tilde{a} and \bar{a} given by (29) and (92), respectively. This relation can be checked by choosing the values of the black hole's parameters shown in Fig.(3) later, and can be used to interpret the formulas of the travel time of the light that in turns generate the relativistic images due to the black holes in a more geometric way in terms of the impact parameter b_{sc} of the light sphere.

It is clear that the coefficient \tilde{b} in (30) has strong dependence of the distance of the observer and the source measured from the black hole, where $Z_{obs} = 1 - r_0/R_{obs} \rightarrow 1$ and $Z_{src} = 1 - r_0/R_{src} \rightarrow 1$ for $R_{obs}, R_{src} \gg r_0$. In particular, \tilde{b} is mainly dominated by $1/(1-Z)$ and $\log(1-Z)$ evaluated at the locations of the source and the observer, respectively. Those main contributions can be understood from the integrand (13) due to the dependence of $1/(1-z)^2$ and $1/(1-z)$. In the observation of the time delay between relativistic images, the difference in \tilde{b} given by two distinct trajectories of the light rays, i.e. $\Delta\tilde{b}$ becomes relevant. In the case of the Schwarzschild black holes by sending $a \rightarrow 0$ in (30), since \tilde{b} just depends on the distance of the observer and the source from the black hole, $\Delta\tilde{b} = 0$. However, as for the Kerr black holes, the contributions of the large $1/(1-Z)$ terms in \tilde{b} from the distinct trajectories of the light rays are canceled so that $\Delta\tilde{b}$ depends only on the black hole's parameters.

In what follows, two interesting limits on the spin of the black hole a , namely $a \rightarrow 0$ and $a \rightarrow M$ are considered to obtain the approximate expressions of \tilde{a} and \tilde{b} . In the small a limit, to its first order, $r_{sc} \simeq 3M - 2\sqrt{3}M/3 \left(\frac{sa}{M}\right) + \mathcal{O}\left(\frac{a}{M}\right)^2$, $b_{sc} \simeq 3\sqrt{3}M - 2M \left(\frac{sa}{M}\right) + \mathcal{O}\left(\frac{a}{M}\right)^2$, $C_{-sc} \simeq \mathcal{O}\left(\frac{a}{M}\right)^3$, $C_{+sc} \simeq 2/3 + 2\sqrt{3}/27 \left(\frac{sa}{M}\right) + \mathcal{O}\left(\frac{a}{M}\right)^3$, and $\tilde{C}_{-sc}/M^2 \simeq \mathcal{O}\left(\frac{a}{M}\right)^3$, $\tilde{C}_{+sc}/M^2 \simeq$

$2\sqrt{3} \left(\frac{sa}{M}\right) + \mathcal{O}\left(\frac{a}{M}\right)^2$, giving

$$\bar{a} \simeq 1 + \frac{2\sqrt{3}}{9} \left(\frac{sa}{M}\right) + \mathcal{O}\left(\frac{a}{M}\right)^2, \quad (35)$$

$$\begin{aligned} \bar{b} &\simeq -\pi + \log[216(7 - 4\sqrt{3})] \\ &\quad + \frac{2}{3\sqrt{3}} \left(1 + \log[216(7 - 4\sqrt{3})] + \frac{3\sqrt{3}}{2} \log \frac{216(7 - 4\sqrt{3})}{72}\right) \left(\frac{sa}{M}\right) + \mathcal{O}\left(\frac{a}{M}\right)^2, \end{aligned} \quad (36)$$

$$\frac{\tilde{a}}{M} \simeq \frac{3\sqrt{3}}{2} + \frac{17\sqrt{3}}{18} \left(\frac{a}{M}\right)^2 + \mathcal{O}\left(\frac{a}{M}\right)^3, \quad (37)$$

$$\begin{aligned} \frac{\tilde{b}}{M} &\simeq \frac{R}{M} + 2 \log \left[(26 - 15\sqrt{3}) \left(3 + 2\frac{R}{M}\right) \right] - 3\sqrt{3} \left[1 + \log \left(\frac{2\sqrt{6} + 3\sqrt{2}}{36} \right) \right] \\ &\quad + \left(\frac{sa}{M}\right) + \mathcal{O}\left(\frac{a}{M}\right)^2. \end{aligned} \quad (38)$$

Since the time delay between two relativistic images depends on the difference in \tilde{b} , for both light rays traveling along either direct or retrograde orbits, $\Delta\tilde{b} = 0$ and for one light ray along the direct orbit and the other along the retrograde orbit $\Delta\tilde{b} = \tilde{b}(a) - \tilde{b}(-a)$ becomes

$$\frac{\Delta\tilde{b}}{M} = \frac{\tilde{b}(a)}{M} - \frac{\tilde{b}(-a)}{M} \simeq 2 \left(\frac{a}{M}\right) + \mathcal{O}\left(\frac{a}{M}\right)^2. \quad (39)$$

To the order of a/M , the dependence of R is removed, and $\Delta\tilde{b}$ has the linear dependence in a , solely depending on the black hole's parameters.

As $a \rightarrow M$ in the extreme black hole, the corresponding event horizon collapse to $r_{\pm} = M$ and the radius of the light sphere turns out to be the same as the event horizon $r_{+c} = M$. The extremely strong gravitational effects in the direct orbits will dramatically affect the time delay observations as compared with the retrograde orbits, where the radius of the light sphere is large than the event horizon, $r_{-c} = 4M > r_{\pm}$. It deserves more efforts to find the approximate expressions of \tilde{a} , \tilde{b} and \bar{a} , \bar{b} in the extreme black hole by introducing a small parameter $\epsilon = 1 - a/M$. For $\epsilon \rightarrow 0$, $r_{sc}r_{\pm} - a^2 \simeq \mathcal{O}(\sqrt{\epsilon})$, $C_{-sc} \simeq 1/2 - \sqrt{3}/4 + \mathcal{O}(\sqrt{\epsilon})$, $C_{+sc} \simeq 1/2 + \sqrt{3}/4 + \mathcal{O}(\sqrt{\epsilon})$, $\tilde{C}_{-sc}/M^2 \simeq -\sqrt{2}/4/\sqrt{\epsilon} + (1 - 2/\sqrt{3}) + \mathcal{O}(\sqrt{\epsilon})$, and $\tilde{C}_{+sc}/M^2 \simeq \sqrt{2}/4/\sqrt{\epsilon} + (1 + 2/\sqrt{3}) + \mathcal{O}(\sqrt{\epsilon})$ for $s = +1$ in the direct orbits. As long as $\sqrt{\epsilon} < 1 - Z = M/R \ll 1$, where R denotes the distance of either the source or the observer measured from the black hole, the behavior of the coefficients \tilde{a} , \tilde{b} , \bar{a} and \bar{b} near the extreme

black holes is found to be

$$\bar{a} \simeq \frac{1}{\sqrt{2}\sqrt{\epsilon}} + \frac{11\sqrt{3}}{6} + \mathcal{O}(\sqrt{\epsilon}) , \quad (40)$$

$$\bar{b} \simeq \frac{1}{\sqrt{2}\sqrt{\epsilon}} \left[\log \left(\frac{3\sqrt{6}}{8} \sqrt{\epsilon} \right) - \frac{6 \ 192 \ 495 \ 697 \ 115 \ 372}{5 \ 636 \ 787 \ 964 \ 422 \ 615} \right] + \frac{25\sqrt{3}}{36} \log(\epsilon) + \mathcal{O}(\text{const.}) \quad (41)$$

$$\frac{\tilde{a}}{M} \simeq \frac{1}{\sqrt{2}\sqrt{\epsilon}} + 7\sqrt{3} + \mathcal{O}(\sqrt{\epsilon}) , \quad (42)$$

$$\begin{aligned} \frac{\tilde{b}}{M} \simeq & \frac{1}{\sqrt{2}\sqrt{\epsilon}} \left[\log \left(\frac{3\sqrt{6}}{8} \sqrt{\epsilon} \right) - \frac{6 \ 192 \ 495 \ 697 \ 115 \ 372}{5 \ 636 \ 787 \ 964 \ 422 \ 615} \right] + \frac{55}{48\sqrt{3}} \log(\epsilon) \\ & + \frac{R}{M} + 2 \log \left(\frac{R}{M} \right) + \mathcal{O}(\text{const.}) . \end{aligned} \quad (43)$$

Again, since $r_{\pm} = r_{+c} = M$ for direct orbits when $a \rightarrow M$, the strong gravitational effects on the light rays drive the values of \bar{a} , $|\bar{b}|$, \tilde{a} and $|\tilde{b}|$ to infinity in the way that the ratio \tilde{a}/\bar{a} remains finite.

For the case of $s = -1$ along the retrograde orbits, the corresponding $r_{-c} = 4M$ when $a \rightarrow M$ is larger than the event horizon $r_{\pm} = M$. The relevant coefficients are approximately by $C_{-sc} \simeq -9\sqrt{2}/112/\sqrt{\epsilon} + 2/7 + \mathcal{O}(\sqrt{\epsilon})$, $C_{+sc} \simeq 9\sqrt{2}/112/\sqrt{\epsilon} + 2/7 + \mathcal{O}(\sqrt{\epsilon})$, and $\tilde{C}_{-sc}/M^2 \simeq 17\sqrt{2}/16/\sqrt{\epsilon} - 2 + \mathcal{O}(\sqrt{\epsilon})$, $\tilde{C}_{+sc}/M^2 \simeq -17\sqrt{2}/16/\sqrt{\epsilon} - 2 + \mathcal{O}(\sqrt{\epsilon})$. Near the extreme black hole,

$$\bar{a} \simeq \frac{4}{3\sqrt{3}} + \mathcal{O}(\epsilon) , \quad (44)$$

$$\bar{b} \simeq -\pi + \frac{1}{9} \left[-6 + 8\sqrt{3} + 4\sqrt{3} \log \left(\frac{1152}{7} (7 - 4\sqrt{3}) \right) \right] + \mathcal{O}(\epsilon) , \quad (45)$$

$$\frac{\tilde{a}}{M} \simeq \frac{14}{3\sqrt{3}} + \mathcal{O}(\epsilon) , \quad (46)$$

$$\frac{\tilde{b}}{M} \simeq \frac{R}{M} + 2 \log \left(\frac{2 - \sqrt{3}}{2} \frac{R}{M} \right) + \mathcal{O}(\sqrt{\epsilon}) . \quad (47)$$

All of them are finite as expected.

We will show later that the time delay from two distinct orbits circling around the extreme black hole will depend on \tilde{a}/\bar{a} , \bar{b} and $\Delta\tilde{b}$. Thus, in addition to \tilde{a} and \tilde{b} , \bar{a} and \bar{b} given by (92) and (93) are also very relevant to the time delay calculations. Notice that with the parameters under investigation $\bar{a} > 0$, but $\bar{b} < 0$. Our results are shown in [22], where both \bar{a} and $|\bar{b}|$ increase (decrease) in a in direct (retrograde) orbits, giving the fact that the deflection angle $\hat{\alpha}$ decreases (increases) with the increase of the black hole's spin for a given

impact parameter. In Fig.(2), the behavior of \bar{b} as a function of a is also drawn emphasizing that as $a \rightarrow M$ in the extreme black hole cases for the direct orbit $|\bar{b}| \propto (1/\sqrt{\epsilon}) \log[1/\sqrt{\epsilon}]$ as $\epsilon \rightarrow 0$ whereas for the retrograde orbit, \bar{b} remains a finite value, consistent with our analytical analysis above in (41) and (45). Fig.(3) is plotted for the ratio of \tilde{a}/\bar{a} that decreases with a for direct orbits but increases in steady for retrograde orbits. Both of them reach a finite value as $a \rightarrow M$. The behavior of \tilde{a}/\bar{a} can be interpreted through the relation $2\tilde{a}/\bar{a} = b_{sc}$ as seen in Fig.(3). In fact, in the Kerr case, given the effective potential W_{eff} in (8) we have stated that the nonzero spin of the black holes induces more repulsive effects to the light rays in the direct orbits than in the retrograde orbits so as to decrease b_{+c} but to increase b_{-c} as a increases. Also, $\Delta\tilde{b} = \tilde{b}(+a) - \tilde{b}(-a)$ between the direct orbit and the retrograde orbit is plotted in Fig.(4) where for small a , $\Delta\tilde{b}$ increases with a consistent with (39), and then goes to $-\infty$ mainly resulting from strong gravitational time delay effects in the direct orbits with $\tilde{b}(+a) \propto (1/\sqrt{\epsilon}) \log[\sqrt{\epsilon}]$ for small ϵ in (43).

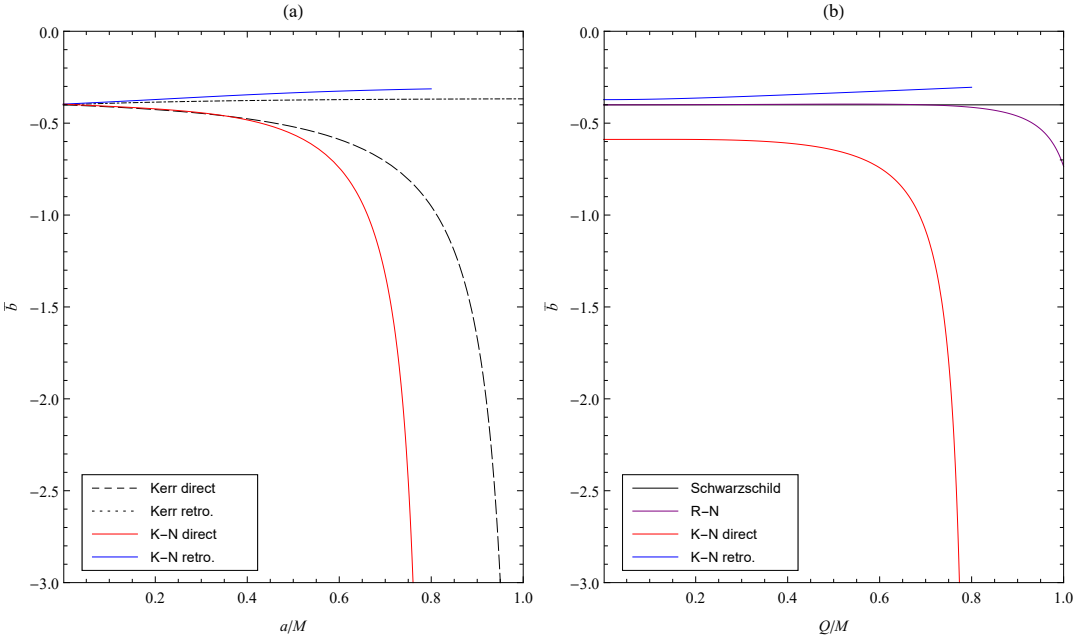


FIG. 2: The behavior of the coefficient \bar{b} against the spin parameter a/M and the black hole charge Q/M . The left and right panels show the cases of Kerr-Newman black holes with $Q/M = 0.6$ and $a/M = 0.6$, respectively. The coefficient \bar{b} of the Kerr, Reissner-Nordström, and Schwarzschild black holes are also shown for comparison.

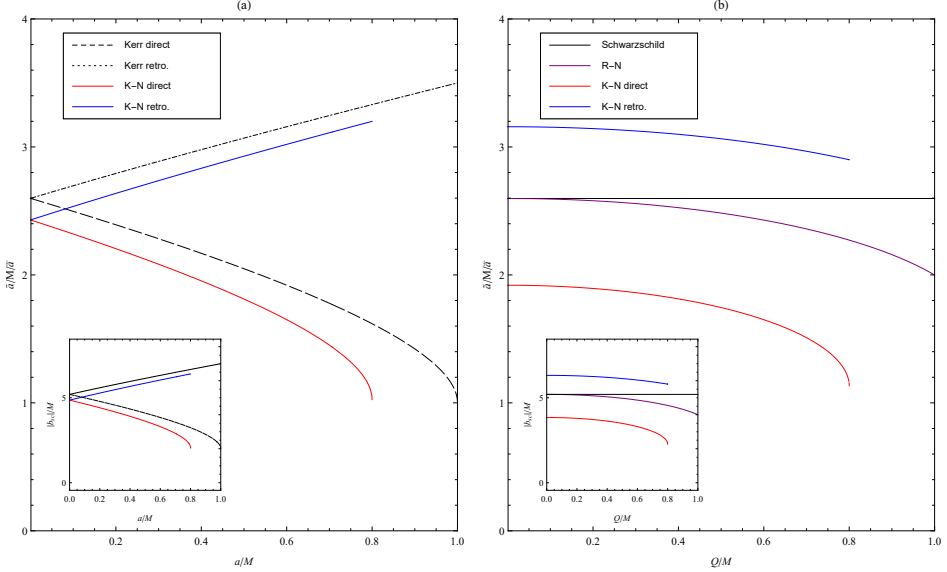


FIG. 3: The ratio $\tilde{a}/M/\bar{a}$ as a function of the spin parameter a/M and the black hole charge Q/M . The left and right panels show the cases of Kerr-Newman black holes with $Q/M = 0.6$ and $a/M = 0.6$, respectively. The cases for Kerr, Reissner-Nordström, and Schwarzschild black holes are shown for comparison. The insets show b_{sc} versus a/M and Q/M for comparison.

B. Kerr-Newman black holes

Another example with the nonspherically symmetric metric that we would like to explore is the Kerr-Newman metric of a charged spinning black hole. With an addition of charge Q comparing with the Kerr case, the line element associated with the Kerr-Newman metric is

$$\begin{aligned} ds^2 &= g_{\mu\nu}dx^\mu dx^\nu \\ &= -\frac{(\Delta - a^2 \sin^2 \theta)}{\Sigma} dt^2 + \frac{a \sin^2 \theta (Q^2 - 2Mr)}{\Sigma} (dt d\phi + d\phi dt) \\ &\quad + \frac{\Sigma}{\Delta} dr^2 + \Sigma d\theta^2 + \frac{\sin^2 \theta}{\Sigma} ((r^2 + a^2)^2 - a^2 \Delta \sin^2 \theta) d\phi^2, \end{aligned} \quad (48)$$

where

$$\Sigma = r^2 + a^2 \cos^2 \theta, \quad \Delta = r^2 + a^2 + Q^2 - 2Mr. \quad (49)$$

The outer (inner) event horizon r_+ (r_-) is

$$r_\pm = M \pm \sqrt{M^2 - (Q^2 + a^2)} \quad (50)$$

with $M^2 > Q^2 + a^2$.

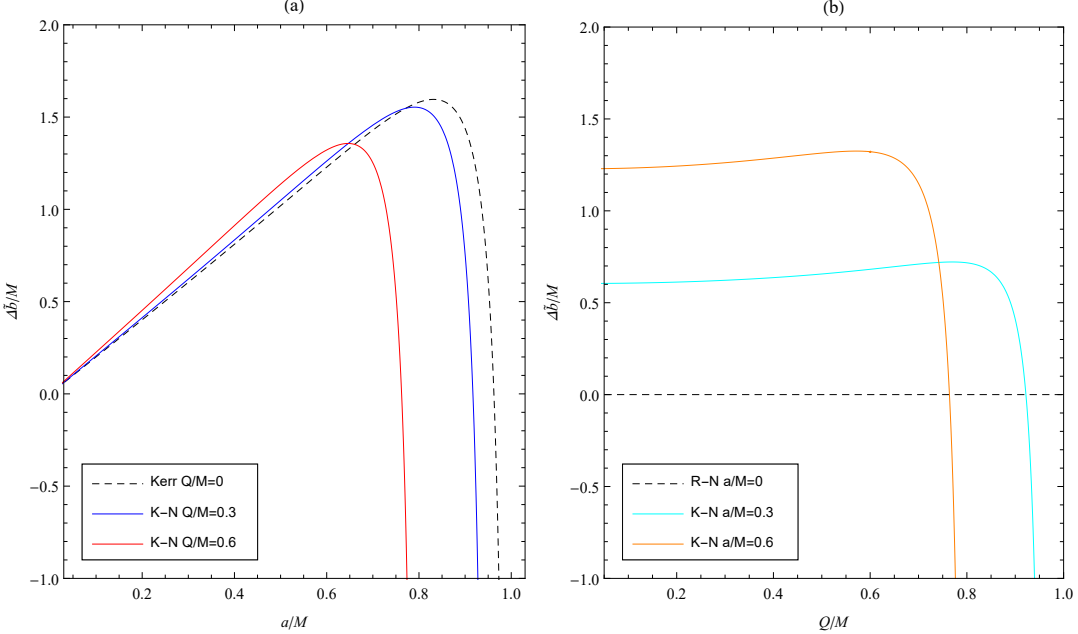


FIG. 4: The difference $\tilde{b}(a) - \tilde{b}(-a)$ versus the spin parameter a/M and the black hole charge Q/M . Plot (a) shows the cases $Q/M = 0.3$ (blue line) and $Q/M = 0.6$ (red line) for Kerr-Newman black holes. The result of the Kerr black hole (dashed line) is also shown for comparison. Plot (b) shows the results of $a/M = 0.3$ (cyan line) and $a = 0.6$ (orange line) for Kerr-Newman black holes. The result of the Reissner-Nordström (dashed line) is shown for comparison.

The light rays traveling on the equatorial plane of the Kerr-Newman black hole have been studied analytically in [22], in which the corresponding function W_{eff} is obtained as

$$W_{\text{eff}}(r) = \frac{1}{r^2} \left[1 - \frac{a^2}{b^2} + \left(-\frac{2M}{r} + \frac{Q^2}{r^2} \right) \left(1 - \frac{a}{b_s} \right)^2 \right]. \quad (51)$$

The nonzero charge of the black hole give repulsive effects to light rays as seen from the $1/r^4$ term, which shifts the innermost circular trajectories of the light toward the black holes with the smaller critical impact parameter b_{sc} for both direct and retrograde orbits, leading to the smaller radius of the light sphere r_{sc} . The travel time of the light crucially depends not only on the locations of the source and the observer but also on the radius of the light sphere circling around the black hole.

The equation of motion for the light rays in terms of the variable z similar to (13) in the

Kerr case is obtained as

$$\frac{dt}{dz} = \frac{r_0}{(1-z)^2} \left[\frac{a(1-\frac{a}{b})(1-z)^3(-\frac{2M}{r_0} + \frac{Q^2}{r_0^2}(1-z)) + \frac{r_0^2}{b} + \frac{a^2}{b}(1-z)^2}{1 - \frac{2M}{r_0}(1-z) + \frac{a^2+Q^2}{r_0^2}(1-z)^2} \right] \frac{1}{\sqrt{B(z, r_0)}}, \quad (52)$$

where

$$B(z, r_0) = c_1(r_0)z + c_2(r_0)z^2 + c_3(r_0)z^3 + c_4(r_0)z^4. \quad (53)$$

The function $B(z, r_0)$ is a quartic polynomial in z with the coefficients

$$c_1(r_0) = 4Q^2 \left(1 - \frac{a}{b_s}\right)^2 - 6Mr_0 \left(1 - \frac{a}{b_s}\right)^2 + 2r_0^2 \left(1 - \frac{a^2}{b^2}\right), \quad (54)$$

$$c_2(r_0) = -6Q^2 \left(1 - \frac{a}{b_s}\right)^2 + 6Mr_0 \left(1 - \frac{a}{b_s}\right)^2 - r_0^2 \left(1 - \frac{a^2}{b^2}\right), \quad (55)$$

$$c_3(r_0) = 4Q^2 \left(1 - \frac{a}{b_s}\right)^2 - 2Mr_0 \left(1 - \frac{a}{b_s}\right)^2, \quad (56)$$

$$c_4(r_0) = -Q^2 \left(1 - \frac{a}{b_s}\right)^2. \quad (57)$$

All coefficients have the additional dependence of the black hole charge Q . The presence of the z^4 term with the coefficient $c_4(r_0)$, which vanishes in the Kerr case, make the expressions of \tilde{a} and \tilde{b} more lengthy.

The integrand $f(z, r_0)$ in (23) now takes the form

$$f(z, r_0) = \frac{r_0}{b} \frac{r_0^2}{a^2 + Q^2} \left[\frac{\tilde{C}_-}{z - z_-} + \frac{\tilde{C}_Q z + \tilde{C}_+}{z - z_+} + \frac{r_0^2}{(1-z)^2(z - z_-)(z - z_+)} \right] \times \frac{1}{\sqrt{c_1(r_0)z + c_2(r_0)z^2 + c_3(r_0)z^3 + c_4(r_0)z^4}}. \quad (58)$$

The corresponding coefficients \tilde{C}_- , \tilde{C}_Q , \tilde{C}_+ in the Kerr-Newman case are

$$\tilde{C}_- = \frac{-2aMbr_- + a^2(a^2 + Q^2) + 2a^2Mr_- + a(b - a)\frac{Q^2}{r_0^2}\frac{r_0^2r_-^2}{a^2+Q^2}}{2r_0\sqrt{M^2 - a^2 - Q^2}}, \quad (59)$$

$$\tilde{C}_Q = \frac{aQ^2}{r_0^2} \left(1 - \frac{a}{b_s}\right) b, \quad (60)$$

$$\tilde{C}_+ = \frac{2aMbr_+ - a^2(a^2 + Q^2) - 2a^2Mr_+ + a(a - b)\frac{Q^2}{r_0^2}(-r_0r_- + r_0r_+ + \frac{r_0^2}{a^2+Q^2}r_-r_+)}{2r_0\sqrt{M^2 - a^2 - Q^2}} \quad (61)$$

Also z_+ , z_- now become

$$z_- = 1 - \frac{r_0r_-}{a^2 + Q^2}, \quad (62)$$

$$z_+ = 1 - \frac{r_0r_+}{a^2 + Q^2}, \quad (63)$$

defined in terms of the outer(inner) black hole horizon r_+ (r_-). Again, $z_\pm \leq 0$ for all a and Q with the nonzero r_+ . Note that, for charge $Q \rightarrow 0$, \tilde{C}_Q vanishes.

Following the previous study of the Kerr black holes, we define the function $f_D(z, r_0)$ as

$$f_D(z, r_0) = \frac{r_0^3}{b(a^2 + Q^2)} \left[\frac{\tilde{C}_-}{z - z_-} + \frac{\tilde{C}_Q z + \tilde{C}_+}{z - z_+} + \frac{r_0^2}{(1 - z)^2(z - z_-)(z - z_+)} \right] \frac{1}{\sqrt{c_1 z + c_2 z^2}}, \quad (64)$$

and its integration over z gives \tilde{a} and \tilde{b}_D in this case. Also, $f_R(z, r_0) = f(z, r_0) - f_D(z, r_0)$ and the corresponding integral of f_R leads to \tilde{b}_R . Finally, the coefficients \tilde{a} and \tilde{b} in the Kerr-Newman case become

$$\tilde{a} = \frac{r_{sc}^3}{2b_{sc}\sqrt{c_{2sc}}} \left[\frac{2M + r_{sc}}{2r_{sc}} + \frac{\tilde{C}_{-sc}}{r_{sc}r_- - a^2 - Q^2} + \frac{(a^2 + Q^2)^3}{r_-^2(r_{sc}r_- - a^2 - Q^2)r_{sc}(r_+ - r_-)} \right] + (- \leftrightarrow +) \quad (65)$$

and

$$\begin{aligned} \tilde{b} = & \frac{1}{2} \tilde{a} \log \left[\frac{8c_{2sc}^2 Z^2 b_{sc}''}{c_{1sc}^2 b_{sc}} \right] \\ & + \frac{r_0^3}{2b\sqrt{c_2}} \left[\frac{\sqrt{3}\sqrt{(3-2Z)+(-4Z+3Z^2)(c_4/c_2)}}{(1-c_4/c_2)(1-Z)} \right. \\ & + \frac{2\sqrt{3}M}{r_0\sqrt{1-c_4/c_2}} \log \left(\frac{(2-Z)(1-c_4/c_2) + \sqrt{1-c_4/c_2}\sqrt{(3-2Z)+(-4Z+3Z^2)(c_4/c_2)}}{2(1-c_4/c_2) + \sqrt{3}\sqrt{1-c_4/c_2}} \frac{1}{1-Z} \right) \\ & \left. - \frac{3}{(1-c_4/c_2)} - \frac{r_0^2}{(a^2 + Q^2 - 2Mr_0 + r_0^2)} \log \tilde{N}(Z, a, Q) \right] \\ & + \frac{r_0^3}{b\sqrt{c_2}} \frac{\tilde{C}_-}{a^2 + Q^2 - r_0 r_-} \left[\log \tilde{N}(Z, a, Q) - \frac{\sqrt{3}(a^2 + Q^2)}{\tilde{W}_-} \log \tilde{M}(Z, a, Q, r_-) \right] \\ & - \frac{r_0^2}{b\sqrt{c_2}} \frac{\sqrt{3}(a^2 + Q^2)^4}{(a^2 + Q^2 - r_0 r_-)r_-^2(r_+ - r_-)\tilde{W}_-} \log \tilde{M}(Z, a, Q, r_-) + (- \leftrightarrow +) \\ & + \frac{r_0^3}{b\sqrt{c_2}} \frac{\sqrt{3}\tilde{C}_Q}{\tilde{W}_+} \log \tilde{M}(Z, a, Q, r_+) \Big|_{r_0=r_{sc}}, \end{aligned} \quad (66)$$

where

$$\tilde{M}(Z, a, Q, r_\pm) = \frac{a^2 + Q^2 - r_0 r_\pm}{(a^2 + Q^2)(1 - Z) - r_0 r_\pm} \frac{\tilde{A}}{\tilde{B}}, \quad (67)$$

$$\begin{aligned} \tilde{A} = & (2 - Z)(a^2 + Q^2) + r_0 r_\pm + [(-2 + Z)(a^2 + Q^2) + (2 - 3Z)r_0 r_\pm] \frac{c_4}{c_2} \\ & + \sqrt{(3 - 2Z) + (-4Z + 3Z^2)} \frac{c_4}{c_2} \tilde{W}_\pm, \end{aligned} \quad (68)$$

$$\tilde{B} = 2(a^2 + Q^2) + r_0 r_\pm - 2(a^2 + Q^2 + r_0 r_\pm) \frac{c_4}{c_2} + \sqrt{3} \tilde{W}_\pm \quad (69)$$

with

$$\tilde{W}_\pm^2 = (a^2 + Q^2 + 2r_0r_\pm)(a^2 + Q^2) - (a^2 + Q^2 + 3r_0r_\pm)(a^2 + Q^2 - r_0r_\pm) \frac{c_4}{c_2} \quad (70)$$

and

$$\tilde{N}(Z, a, Q) = \frac{(3 - Z) - 2Z(c_4/c_2) + \sqrt{3}\sqrt{(3 - 2Z) + (-4Z + 3Z^2)(c_4/c_2)}}{6}. \quad (71)$$

In the equations above, we have replaced c_{3sc} by the linear combination of c_{2sc} and c_{4sc} with

$$c_{3sc} = -\frac{2}{3}c_{2sc} - \frac{4}{3}c_{4sc}. \quad (72)$$

Now we consider the limit of $a \rightarrow 0$ for the Reissner-Nordström black hole with the spherical symmetry metric. As $a \rightarrow 0$, $\tilde{C}_{\pm sc} \rightarrow 0$ and $c_{2sc} = 3Mr_c - 4Q^2$ given by the known equation for the radius of the light sphere $r_c^2 = -2Q^2 + 3Mr_c$ [15]. Straightforward calculations lead to

$$\tilde{a} = \frac{r_c^2}{2b_c\sqrt{3Mr_c - 4Q^2}} \left[2M + r_c + \frac{2MQ^2 - 4M^2r_c + Q^2r_c}{Q^2 - Mr_c} \right] \quad (73)$$

where we have used the formulas of the critical radius

$$r_c = \frac{3M + \sqrt{9M^2 - 8Q^2}}{2}, \quad (74)$$

and the critical impact parameter

$$b_c = \frac{r_c^2}{\sqrt{Mr_c - Q^2}}. \quad (75)$$

Recalling the coefficient \bar{a} for the Reissner-Nordström case

$$\bar{a} = \frac{r_c}{\sqrt{3Mr_c - 4Q^2}}, \quad (76)$$

the expected relation in (34) can be achieved for the spherically symmetric black hole. As for the Kerr-Newman black holes, although the analytic expressions of \tilde{a} in (65), \bar{a} in (105) and b_{sc} in (104) are so complicated, it is quite straightforward to find that the relation is amazingly fulfilled in the Kerr-Newman black holes, which can be further justified by putting in the black hole's parameters shown in Fig.(3). This is one of the interesting findings in this work. Again, the relation (34) can provide more geometric interpretation to the formula of the time delay to be developed later.

As $Q \rightarrow 0$, \tilde{C}_Q and $c_4 \rightarrow 0$. The coefficients \tilde{a} and \tilde{b} in (65) and (66) of the Kerr-Newman black holes reduce to that of the Kerr black holes in (29) and (30), respectively. One of the applications of the analytical expressions of \tilde{a} and \tilde{b} is to find their values with the input of b_{sc} in (100) or r_{sc} in (96) for given black hole's parameters. As in the Kerr case, it is quite interesting to study the limiting cases of either $a \rightarrow 0$ or $a \rightarrow \sqrt{M^2 - Q^2}$, with which to analytically understand the time delay effects. We find that, in both limits, \tilde{a} , \tilde{b} , \bar{a} and \bar{b} follow the same expansion behavior as in (35)-(38) when $a \rightarrow 0$ and (40)-(47) when $a \rightarrow \sqrt{M^2 - Q^2}$ with the additional dependence on the charge Q in the expansion coefficients. Nevertheless, the expressions of those coefficients are too lengthy to show them here. With that features in both limits allows us to see the charge Q effects in Figs (2),(3) and (4). Due to the fact that the bending angle for light rays resulting from the charged black hole is suppressed as compared with the neutral black hole with the same impact parameter b and the angular momentum of the black holes a , both \bar{a} in (105) and $|\bar{b}|$ in (106) are found to increase with the charge Q shown in our previous paper [22] and also in Fig.(2) depicting the coefficient \bar{b} . In Fig.(2), with fixed Q , for the direct orbit $|\bar{b}|$ increases with a and then reaches infinity as the spin reaches its extreme value, $a \rightarrow \sqrt{M^2 - Q^2}$ and for the retrograde orbit, $|\bar{b}|$ decreases with a all the way to a finite value in the extreme black holes as in the Kerr cases in (41) and (45). In Fig.(3), given Q the ratio \tilde{a}/\bar{a} behaves the same as in the Kerr cases except that the largest value of a can be $a = \sqrt{M^2 - Q^2}$ in the extreme black holes. Since the nonzero charge of the black hole give repulsive effects to light rays giving that b_{sc} decreases with Q for both direct and retrograde orbits, the parameter \tilde{a}/\bar{a} due to the relation (34) also decreases with Q . Fig.(4) shows $\Delta\tilde{b}$ as a function of Q (a) with a fixed a (Q) in that $\Delta\tilde{b}$ respectively goes to $-\infty$ in the extreme Kerr-Newman black holes ($\Delta\tilde{b} \propto \log \epsilon$ with $\epsilon = 1 - \sqrt{M^2 + Q^2}/M$ in the small ϵ limit) as in the extreme Kerr black holes. In the next section we will see how the charge Q of the black hole affects the time delay observations.

III. TIME DELAY DUE TO GRAVITATIONAL LENS OF SUPERMASSIVE GALACTIC BLACK HOLES

We now derive the formulas of the time delay between two relativistic images based upon (2) as well as the angular positions of those images obtained in [20]. The angular positions

of the source and the image are measured from the optical axis, and are denoted by β and θ , respectively (see [20] for detail). The lens equation as the light rays travel around the black hole n times can be simplified as

$$s\beta \simeq \theta - \frac{d_{LS}}{d_S}[\hat{\alpha}(\theta) - 2n\pi] \quad (77)$$

with the relation between the impact parameter b and the angular position of the image approximated by

$$b \simeq d_L \theta. \quad (78)$$

According to [20], the zeroth order solution θ_{sn}^0 is obtained from $\hat{\alpha}(\theta_{sn}^0) = 2n\pi$. Using the SDL deflection angle in (11) we have then

$$\theta_{sn}^0 = \frac{|b_{sc}|}{d_L} \left(1 + e^{\frac{\bar{b}-2n\pi}{\bar{a}}} \right) \quad (79)$$

for $n = 1, 2, \dots$. Replacing b by θ via (78) in (2) and substituting the result (79), the travel time in the SDL becomes

$$T_{sn} = \frac{2\tilde{a}(sa)}{\bar{a}(sa)} [2\pi n - \bar{b}(sa)] + \tilde{b}(R_{obs}, sa) + \tilde{b}(R_{src}, sa). \quad (80)$$

We consider that the time delay for two relativistic images lying in the same side of the optic axis where both light rays are along either direct or retrograde orbits with the same sa winding around the black hole n and m times, respectively. Their difference can be obtained as

$$\Delta T_{n,m}^{(s)} = 2\pi(n - m) \frac{2\tilde{a}(\pm a)}{\bar{a}(\pm a)} \quad (81)$$

with the superscript “s” in T . In the other case, when two images are on the opposite side of the optical axis resulting from the light rays circling around the black hole n time in the direct orbit and m times in the retrograde orbit, respectively. The time delay denoted with the superscript “o” then becomes

$$\begin{aligned} \Delta T_{n,m}^{(o)} = & \frac{2\tilde{a}(a)}{\bar{a}(a)} [2\pi n - \bar{b}(a)] + \tilde{b}(R_{obs}, a) + \tilde{b}(R_{src}, a) \\ & - \frac{2\tilde{a}(-a)}{\bar{a}(-a)} [2\pi m - \bar{b}(-a)] - \tilde{b}(R_{obs}, -a) - \tilde{b}(R_{src}, -a). \end{aligned} \quad (82)$$

The formula of the time delay depends on the ratio $2\tilde{a}/\bar{a}$, related to the impact parameter of the light ray for the light sphere b_{sc} through (34), and the number of the loops n for the light

winding around the black hole and the coefficients \bar{b} , that together give the effective winding angle $2\pi n - \bar{b}$. The dependence also involves \tilde{b} with strong dependence of the distances of the source and the observer from the black holes. But the difference $\Delta\tilde{b}$ between two distinct trajectories of the light rays solely depends on the black hole's parameters. Substituting the small a behavior in the Kerr case (35)-(38), the time delays $\Delta T_{n,m}^{(s)}$ and $\Delta T_{n,m}^{(o)}$ can be approximated by

$$\Delta T_{n,m}^{(s)} = 2\pi(n-m)M \left[3\sqrt{3} - 2\left(\frac{sa}{M}\right) + \mathcal{O}\left(\frac{a}{M}\right)^2 \right], \quad (83)$$

$$\begin{aligned} \Delta T_{n,m}^{(o)} = & 3\sqrt{3}M(n-m)\pi + 2M \left[-2(1+n+m)\pi - 3\sqrt{3}\log\left(3(7-4\sqrt{3})\right) \right] \left(\frac{a}{M}\right) \\ & + \mathcal{O}\left(\frac{a}{M}\right)^2. \end{aligned} \quad (84)$$

In the extreme case, following small ϵ expansion in (40)-(47) as $a \rightarrow M$, we get

$$\Delta T_{n,m}^{(s)}(+a) = 2\pi(n-m)M \left[2 + \left(\frac{11\sqrt{6}}{3} - 12\sqrt{6}\right)\sqrt{\epsilon} + \mathcal{O}(\epsilon) \right], \quad (85)$$

$$\Delta T_{n,m}^{(s)}(-a) = 2\pi(n-m)M (14 + \mathcal{O}(\epsilon)), \quad (86)$$

and

$$\Delta T_{n,m}^{(o)} = \left[-\frac{25\sqrt{3}M}{18} + \frac{55M}{24\sqrt{3}} \right] \log(\epsilon) + \mathcal{O}(\text{const.}). \quad (87)$$

The time delay $\Delta T_{n,m}^{(s)}$ given by (81) is determined by \tilde{a}/\bar{a} shown in Fig.(3) for fixed m and n . Due to the relation (34), the decrease (increase) of $b_{+c}(b_{-c})$ as a increases in the direct orbits (the retrograde orbits) lead to the decrease (increase) of the time delay $|\Delta T_{n,m}^{(s)}(+a)|$ ($|\Delta T_{n,m}^{(s)}(-a)|$) as long as $n \neq m$ in agreement with the results of [25]. Here we also find that the effects of the nonzero charge of the black holes decreases $|\Delta T_{n \neq m}^{(s)}(\pm a)|$ for both direct and retrograde orbits because the impact parameter of the innermost circular motion b_{sc} decreases with Q .

When one light ray is along the direct orbit and the other follows retrograde orbits, the time delay $\Delta T_{n,m}^{(o)}$ is plotted in Figs.(5) and (6), in which number of the loops are chosen to be $n = 1$ ($m = 1$) for the direct (retrograde) orbits. For small a , $\Delta T_{1,1}^{(o)}$ is dominated by \tilde{a}/\bar{a} , which follows the relation (34), and since $b_{+c} < b_{-c}$, $\Delta T_{1,1}^{(o)}$ is negative and $|\Delta T_{1,1}^{(o)}|$ increase with a , consistent with [25]. Its linear a dependence can be given by the analytic approximation (84). Nevertheless, in the extreme black holes, the large gravitational effects

to the direct orbits drives $\Delta T_{1,1}^{(o)}$ becoming positive and further more goes to a very large value also consistent with (87). The effects of the charge in steady lead to the larger $|\Delta T_{1,1}^{(o)}|$ for the same a . Near extreme black holes $\Delta T_{1,1}^{(o)} \propto \log \epsilon$, where $\epsilon = 1 - \sqrt{M^2 + Q^2}/M$ in the small ϵ limit. The slope of $\Delta T_{1,1}^{(o)} \rightarrow \infty$ as $\epsilon \rightarrow 0$ for nonzero charge black holes is slightly larger than the Kerr Black holes. Again, the time delay between two relativistic images in the limits of small a as well as $a \rightarrow \sqrt{M^2 - Q^2}$ can be understood from taking the appropriate limits of the obtained analytical expressions of all coefficients.

We now take the examples of a galactic black hole and the supermassive black holes such as Sagittarius A* and M87 [35, 36]. We also assume a light source at the distance with the ratio $d_{LS}/d_S = 1/2$ as shown in Tables (I) and (II) [37–39]. It is evident that the black hole with higher mass or with spin of the extreme black hole will have higher time delay. It has also been emphasized in [25] that the time delay measurement together with the analytical expressions of all coefficients of \bar{a} and \bar{b} in the SDL expression of the deflection angle (11) as well as \tilde{a} and \tilde{b} again in the SDL of the travel time (23) can be used to estimate the properties of the black holes including its distance from the observer.

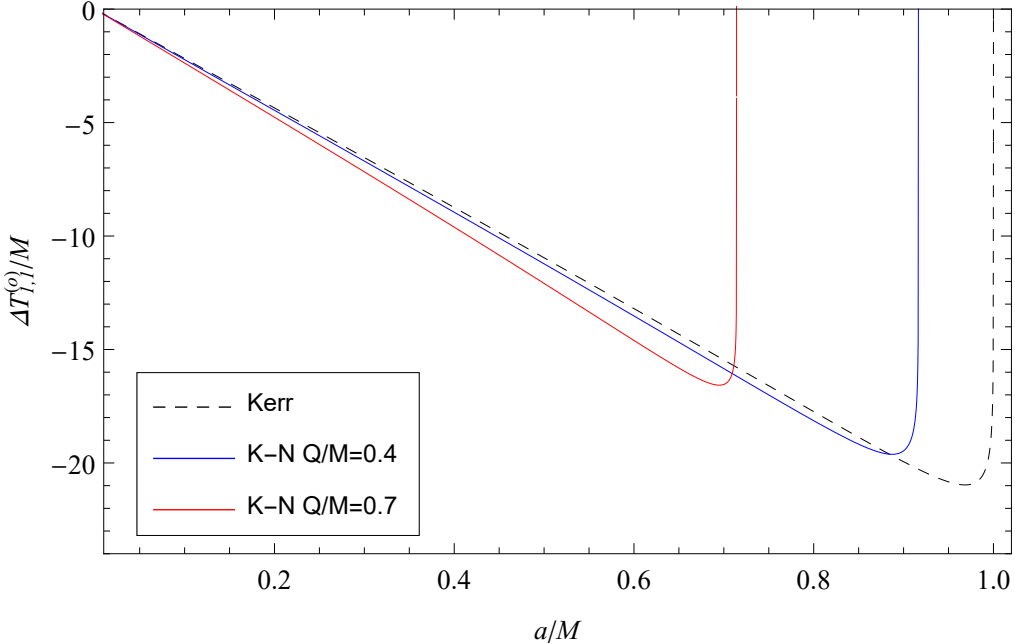


FIG. 5: The time delay $\Delta T_{1,1}^{(o)}$ as a function of the spin parameter a/M with the black hole charge $Q/M = 0$ (dashed line), $Q/M = 0.4$ (blue line), and $Q/M = 0.7$ (red line).

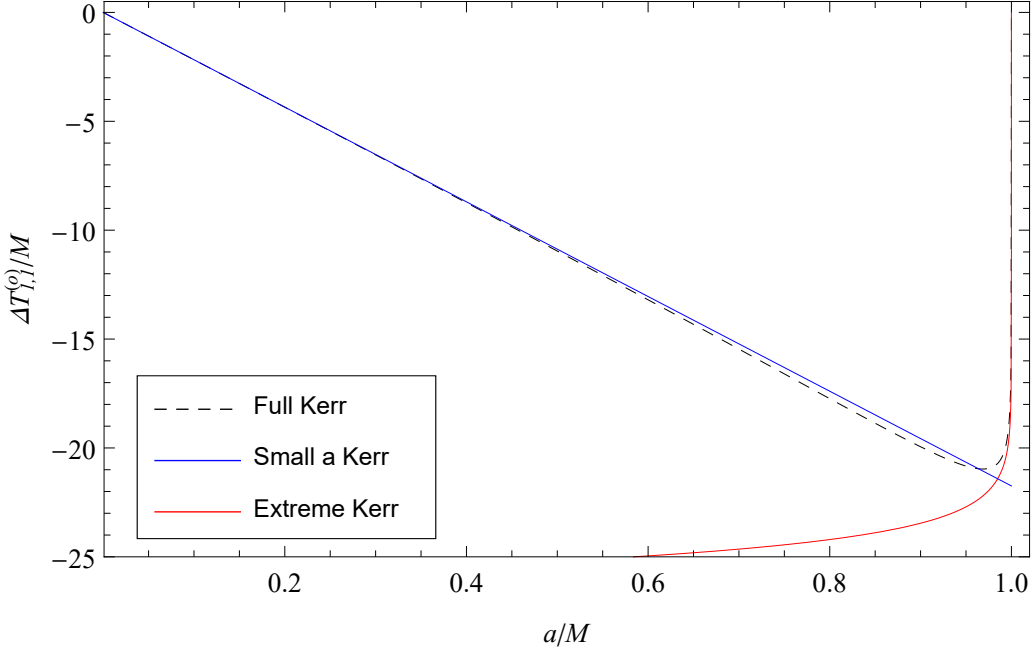


FIG. 6: Plot comparison of the perturbative small $a \rightarrow 0$ expansion (blue line) and the extreme Kerr approximation $a \rightarrow M$ (red line) against the full calculation of $\Delta T_{1,1}^{(o)}$.

	M/M_\odot	sa/M	Q/M	Distance $d_L(Mpc)$	$\Delta T_{2,1}^{(s)}(h)$
Galactic black hole	2.8×10^6	0	0	0.0085	0.125
Sagittarius A*	4.1×10^6	0.1	0	0.0082	0.176
NGC4486 (M87)	3.3×10^9	0.9	0	15.3	80.755
Galactic black hole	2.8×10^6	0	0	0.0085	0.125
Sagittarius A*	4.1×10^6	-0.1	0	0.0082	0.190
NGC4486 (M87)	3.3×10^9	-0.9	0	15.3	193.973

TABLE I: Estimates of the time delay $\Delta T_{2,1}^{(s)}$ for some galactic and supermassive black holes [37–39]. The unit of the time difference h means "hour".

IV. SUMMARY AND OUTLOOK

In summary, we study the time delay between two relativistic images due to strong gravitational lensing caused by the Kerr and Kerr-Newman black holes respectively. Starting from the known form of the SDL deflection angle in (11) with the coefficients \bar{a} and \bar{b} , one can derive the formula for travel time of the light rays from the distant source winding

	M/M_\odot	a/M	Q/M	Distance	$d_L(Mpc)$	$\Delta T_{1,1}^{(o)}(h)$
Galactic black hole	2.8×10^6	0	0		0.0085	0
Sagittarius A*	4.1×10^6	0.1	0		0.0082	-0.012
NGC4486 (M87)	3.3×10^9	0.9	0		15.3	-90.129

TABLE II: Estimates of the time delay $\Delta T_{1,1}^{(o)}$ for some galactic and supermassive black holes [37–39]. The unit of the time difference h means "hour".

around the black hole and reaching the observer, given in (23), with another two coefficients \tilde{a} and \tilde{b} . Here we successfully obtain their analytical expressions and together with the coefficients \bar{a} and \bar{b} , we are able to explore the time delay phenomena. In particular, we find that the relation (34) still holds true in the Kerr and Kerr-Newman black holes that provide a more geometric interpretation to the time delay formulas we develop here. Based upon our analytical and numerical studies, the black hole with higher mass or with spin of the extreme black hole will have higher time delay. The effect of the charge of the black hole reduces the time delay between two relativistic images lying on the same side of the optical axis when both travel along either direct or retrograde orbits. However, when one light ray is in the direct orbit but the other is in the retrograde orbit resulting in the images on the opposite side of the optical axis instead, the charge effect enhances the time delay between them.

Hopefully, relativistic images will be observed in the near future [40, 41]. Through the analytical results we present in this work, one can reconstruct the black hole's parameters that give strong lensing effects. Also, inspired by the recent advent of horizon-scale observations of astrophysical black holes, the properties of null geodesics become of great relevance to astronomy. The recent work of [41–43] provides an extensive analysis on Kerr black holes. We also plan to extend the analysis of null geodesic to Kerr-Newman black holes, focusing on the effects from the charge of black holes.

Acknowledgments

This work was supported in part by the Ministry of Science and Technology, Taiwan, under Grant No.109-2112-M-259-003.

V. APPENDIX A

We summarize the analytical expression of the smallest radius r_{sc} of the circular motion of the light rays and the corresponding impact parameter b_{sc} . We also present here the SDL deflection angle in the form (11) with the coefficients of \bar{a} and \bar{b} for the Kerr and Kerr-Newman black holes, respectively, from our previous paper [20, 22].

A. Kerr black holes

The innermost trajectories of light rays have the smallest radius r_{sc} given by

$$r_{sc} = 2M \left\{ 1 + \cos \left[\frac{2}{3} \cos^{-1} \left(\frac{-sa}{M} \right) \right] \right\} \quad (88)$$

obtained from the equation

$$r_{sc}^2 - 3Mr_{sc} + 2a(Mr_{sc})^{1/2} = 0 \quad (89)$$

with the corresponding impact parameter

$$b_{sc} = -a + s6M \cos \left[\frac{1}{3} \cos^{-1} \left(\frac{-sa}{M} \right) \right]. \quad (90)$$

Combining (88) and (90) leads to

$$b_{sc} = a + \frac{r_{sc}^2}{\sqrt{Mr_{sc}}}. \quad (91)$$

The coefficients \bar{a} and \bar{b} in (11) are

$$\bar{a} = \frac{r_{sc}^3}{\sqrt{c_{2sc}}} \left[\frac{C_{-sc}}{r_{sc}r_- - a^2} + \frac{C_{+sc}}{r_{sc}r_+ - a^2} \right], \quad (92)$$

$$\begin{aligned} \bar{b} = & -\pi + \bar{a} \log \left(\frac{36}{7 + 4\sqrt{3}} \frac{8c_{2sc}^2 b_{sc}''}{c_{1sc}^2 b_{sc}} \right) \\ & + \frac{r_{sc}^3}{\sqrt{c_{2sc}}} \frac{2aC_{-sc}}{a^2 - r_{sc}r_-} \frac{\sqrt{3}}{\sqrt{a^2 + 2r_{sc}r_-}} \log \left(\frac{\sqrt{a^2 + 2r_{sc}r_-} - a}{\sqrt{a^2 + 2r_{sc}r_-} + a} \frac{\sqrt{a^2 + 2r_{sc}r_-} + \sqrt{3}a}{\sqrt{a^2 + 2r_{sc}r_-} - \sqrt{3}a} \right) \\ & + \frac{r_{sc}^3}{\sqrt{c_{2sc}}} \frac{2aC_{+sc}}{a^2 - r_{sc}r_+} \frac{\sqrt{3}}{\sqrt{a^2 + 2r_{sc}r_+}} \log \left(\frac{\sqrt{a^2 + 2r_{sc}r_+} - a}{\sqrt{a^2 + 2r_{sc}r_+} + a} \frac{\sqrt{a^2 + 2r_{sc}r_+} + \sqrt{3}a}{\sqrt{a^2 + 2r_{sc}r_+} - \sqrt{3}a} \right), \end{aligned} \quad (93)$$

where z_- , z_+ are defined in (19), and the coefficients C_- , C_+ are

$$C_- = \frac{a^2 - 2Mr_-(1 - \frac{a}{b_s})}{2r_0\sqrt{M^2 - a^2}}, \quad (94)$$

$$C_+ = \frac{-a^2 + 2Mr_+(1 - \frac{a}{b_s})}{2r_0\sqrt{M^2 - a^2}} \quad (95)$$

with r_+ (r_-) being the outer (inner) horizon of a Kerr black hole defined in (5) and c_1, c_2, c_3 are given by (15)-(17).

B. Kerr-Newman black holes

As for the Kerr-Newman black hole, the solution of r_{sc} of the radius of the innermost circular motion has been found in [22] as

$$r_{sc} = \frac{3M}{2} + \frac{1}{2\sqrt{3}} \sqrt{9M^2 - 8Q^2 + U_c + \frac{P_c}{U_c}} - \frac{s}{2} \sqrt{6M^2 - \frac{16Q^2}{3} - \frac{1}{3} \left(U_c + \frac{P_c}{U_c} \right) + \frac{8\sqrt{3}Ma^2}{\sqrt{9M^2 - 8Q^2 + U_c + \frac{P_c}{U_c}}}} , \quad (96)$$

where

$$P_c = (9M^2 - 8Q^2)^2 - 24a^2(3M^2 - 2Q^2) , \quad (97)$$

$$U_c = \left\{ (9M^2 - 8Q^2)^3 - 36a^2(9M^2 - 8Q^2)(3M^2 - 2Q^2) + 216M^2a^4 + 24\sqrt{3}a^2\sqrt{(M^2 - a^2 - Q^2)[Q^2(9M^2 - 8Q^2)^2 - 27M^4a^2]} \right\}^{\frac{1}{3}} \quad (98)$$

from solving the following equation

$$2Q^2 + r_c^2 - 3Mr_c + 2a(Mr_c - Q^2)^{1/2} = 0 . \quad (99)$$

The analytical expression of the critical value of the impact parameter b_{sc} can be written as a function of black hole's parameters [22],

$$b_{sc} = -a + \frac{M^2a}{2(M^2 - Q^2)} + \frac{s}{2\sqrt{3}(M^2 - Q^2)} \left[\sqrt{V + (M^2 - Q^2) \left(U + \frac{P}{U} \right)} + \sqrt{2V - (M^2 - Q^2) \left(U + \frac{P}{U} \right) - \frac{s6\sqrt{3}M^2a[(M^2 - Q^2)(9M^2 - 8Q^2)^2 - M^4a^2]}{\sqrt{V + (M^2 - Q^2)(U + \frac{P}{U})}}} \right] , \quad (100)$$

where

$$P = (3M^2 - 4Q^2) [9(3M^2 - 4Q^2)^3 + 8Q^2(9M^2 - 8Q^2)^2 - 216M^4a^2] , \quad (101)$$

$$\begin{aligned} U = & \left\{ - [3(3M^2 - 2Q^2)^2 - 4Q^4] [9M^2(9M^2 - 8Q^2)^3 - 8 [3(3M^2 - 2Q^2)^2 - 4Q^4]^2] \right. \\ & + 108M^4a^2 [9(3M^2 - 4Q^2)^3 + 4Q^2(9M^2 - 8Q^2)^2 - 54M^4a^2] \\ & \left. + 24\sqrt{3}M^2\sqrt{(M^2 - a^2 - Q^2)[Q^2(9M^2 - 8Q^2)^2 - 27M^4a^2]^3} \right\}^{\frac{1}{3}} , \end{aligned} \quad (102)$$

$$V = 3M^4a^2 + (M^2 - Q^2) [6(3M^2 - 2Q^2)^2 - 8Q^4] . \quad (103)$$

Corresponding to (91) we have in this case [22]

$$b_{sc} = a + \frac{r_{sc}^2}{\sqrt{Mr_{sc} - Q^2}} . \quad (104)$$

These will serve as the important inputs for the analytical expressions of the coefficients \bar{a} and \bar{b} in (11), where

$$\bar{a} = \frac{r_{sc}^3}{\sqrt{c_{2sc}}} \left[\frac{C_{-sc}}{r_{sc}r_- - (a^2 + Q^2)} + \frac{C_{+sc}}{r_{sc}r_+ - (a^2 + Q^2)} \right] \quad (105)$$

and

$$\begin{aligned} \bar{b} = & -\pi + \bar{a} \log \left[\frac{36}{4(1 - c_{4sc}/c_{2sc})^2 + 4\sqrt{3}(1 - c_{4sc}/c_{2sc})^{3/2} + 3(1 - c_{4sc}/c_{2sc})} \frac{8c_{2sc}^2 b_{sc}''}{c_{1sc}'^2 b_{sc}} \right] \\ & + \frac{r_{sc}^3}{\sqrt{c_{2sc}}} \frac{2(a^2 + Q^2)C_{-sc}}{(a^2 + Q^2 - r_{sc}r_-)P_-} \sqrt{3} \\ & \times \log \left[\frac{-r_{sc}r_-}{a^2 + Q^2 - r_{sc}r_-} \frac{(P_- + \sqrt{3}(a^2 + Q^2))^2 - 3(a^2 + Q^2 - r_{sc}r_-)^2(c_{4sc}/c_{2sc})}{(P_- + (a^2 + Q^2)(1 - c_{4sc}/c_{2sc})^{1/2})^2 - 3r_{sc}^2r_-^2(c_{4sc}/c_{2sc})} \right] \\ & + \frac{r_{sc}^3}{\sqrt{c_{2sc}}} \frac{2[(a^2 + Q^2)C_{+sc} + (a^2 + Q^2 - r_{sc}r_+)C_{Qsc}]\sqrt{3}}{(a^2 + Q^2 - r_{sc}r_+)P_+} \\ & \times \log \left[\frac{-r_{sc}r_+}{a^2 + Q^2 - r_{sc}r_+} \frac{(P_+ + \sqrt{3}(a^2 + Q^2))^2 - 3(a^2 + Q^2 - r_{sc}r_+)^2(c_{4sc}/c_{2sc})}{(P_+ + (a^2 + Q^2)(1 - c_{4sc}/c_{2sc})^{1/2})^2 - 3r_{sc}^2r_+^2(c_{4sc}/c_{2sc})} \right] . \end{aligned} \quad (106)$$

The coefficients c_1, c_2, c_3 , and c_4 are listed in (54)-(57). In the equation above we have defined also

$$P_{\pm}^2 = (a^2 + Q^2 + 2r_{sc}r_{\pm})(a^2 + Q^2) - (a^2 + Q^2 + r_{sc}r_{\pm})(a^2 + Q^2 - r_{sc}r_{\pm}) \frac{c_{4sc}}{c_{2sc}} . \quad (107)$$

The corresponding coefficients C_- , C_Q , and C_+ in the Kerr-Newman case are

$$C_- = \frac{a^2 + Q^2 - 2Mr_-(1 - \frac{a}{b_s}) + \frac{Q^2r_-^2}{a^2+Q^2}(1 - \frac{a}{b_s})}{2r_0\sqrt{M^2 - a^2 - Q^2}}, \quad (108)$$

$$C_Q = \frac{Q^2}{r_0^2} \left(1 - \frac{a}{b_s}\right), \quad (109)$$

$$C_+ = \frac{a^2 + Q^2 - 2Mr_-(1 - \frac{a}{b_s}) + \frac{Q^2}{r_0}(r_+ - r_-)(1 - \frac{a}{b_s}) + Q^2(1 - \frac{a}{b_s})}{-2r_0\sqrt{M^2 - a^2 - Q^2}}. \quad (110)$$

VI. APPENDIX B

The integrals of the function $f_D(z, r_0)$ in (24) and $f_R(z, r_0) = f(z, r_0) - f_D(z, r_0)$ in the Kerr cases are obtained analytically as

$$\begin{aligned} I_D(r_0) &= \int_0^Z f_D(z, r_0) dz \\ &= \frac{r_0^3}{a^2b} \frac{\tilde{C}_-}{\sqrt{c_1z_- + c_2z_-^2}} \log \left(\frac{\sqrt{c_1z_- + c_2z_-Z} + \sqrt{Z}\sqrt{c_1 + c_2z_-}}{\sqrt{c_1z_- + c_2z_-Z} - \sqrt{Z}\sqrt{c_1 + c_2z_-}} \right) \\ &\quad + \frac{r_0^3}{a^2b} \frac{\tilde{C}_+}{\sqrt{c_1z_+ + c_2z_+^2}} \log \left(\frac{\sqrt{c_1z_+ + c_2z_+Z} + \sqrt{Z}\sqrt{c_1 + c_2z_+}}{\sqrt{c_1z_+ + c_2z_+Z} - \sqrt{Z}\sqrt{c_1 + c_2z_+}} \right) \\ &\quad + \frac{r_0^3}{a^2b} \frac{r_0^2}{2\sqrt{c_1 + c_2Z}} \left[-\frac{2\sqrt{Z}(c_1 + c_2Z)}{(c_1 + c_2)(Z - 1)(z_- - 1)(z_+ - 1)} \right. \\ &\quad - \frac{2\sqrt{c_1 + c_2Z}}{(z_- - 1)^2\sqrt{c_1z_- + c_2z_-^2}(z_- - z_+)} \log \left(\frac{\sqrt{c_1z_- + c_2z_-Z} + \sqrt{c_1Z + c_2z_-Z}}{\sqrt{c_1z_- + c_2z_-Z} - \sqrt{c_1Z + c_2z_-Z}} \right) \\ &\quad + \frac{2\sqrt{c_1 + c_2Z}}{(z_+ - 1)^2\sqrt{c_1z_+ + c_2z_+^2}(z_- - z_+)} \log \left(\frac{\sqrt{c_1z_+ + c_2z_+Z} + \sqrt{c_1Z + c_2z_+Z}}{\sqrt{c_1z_+ + c_2z_+Z} - \sqrt{c_1Z + c_2z_+Z}} \right) \\ &\quad + \frac{\sqrt{c_1 + c_2Z}[c_1(5 + z_-(z_+ - 3) - 3z_+) + 2c_2(3 + z_-(z_+ - 2) - 2z_+)]}{(c_1 + c_2)^{3/2}(z_- - 1)^2(z_+ - 1)^2} \log \left(\frac{1 + \sqrt{Z}}{1 - \sqrt{Z}} \right) \\ &\quad + \frac{\sqrt{c_1 + c_2Z}[c_1(5 + z_-(z_+ - 3) - 3z_+) + 2c_2(3 + z_-(z_+ - 2) - 2z_+)]}{(c_1 + c_2)^{3/2}(z_- - 1)^2(z_+ - 1)^2} \\ &\quad \times \left. \log \left(\frac{c_1 + c_2\sqrt{Z} + \sqrt{c_1 + c_2}\sqrt{c_1 + c_2Z}}{c_1 - c_2\sqrt{Z} + \sqrt{c_1 + c_2}\sqrt{c_1 + c_2Z}} \right) \right]. \end{aligned} \quad (111)$$

$$\begin{aligned}
I_R(r_0) &= \int_0^Z f_R(z, r_0) dz \\
&= \frac{r_0}{b} \frac{r_0^2}{a^2} \frac{\tilde{C}_-}{\sqrt{c_2} z_-} \log \left(\frac{z_-}{z_- - Z} \frac{\sqrt{c_2 + c_3 Z} + \sqrt{c_2} c_3 Z}{\sqrt{c_2 + c_3 Z} - \sqrt{c_2} 4c_2} \right) \\
&\quad + \frac{r_0}{b} \frac{r_0^2}{a^2} \frac{\tilde{C}_-}{\sqrt{c_2 + c_3 z_-} z_-} \log \left(\frac{\sqrt{c_2 + c_3 z_-} - \sqrt{c_2 + c_3 Z}}{\sqrt{c_2 + c_3 z_-} + \sqrt{c_2 + c_3 Z}} \frac{\sqrt{c_2 + c_3 z_-} + \sqrt{c_2}}{\sqrt{c_2 + c_3 z_-} - \sqrt{c_2}} \right) \\
&\quad + \frac{r_0}{b} \frac{r_0^2}{a^2} \frac{\tilde{C}_+}{\sqrt{c_2} z_+} \log \left(\frac{z_+}{z_+ - Z} \frac{\sqrt{c_2 + c_3 Z} + \sqrt{c_2} c_3 Z}{\sqrt{c_2 + c_3 Z} - \sqrt{c_2} 4c_2} \right) \\
&\quad + \frac{r_0}{b} \frac{r_0^2}{a^2} \frac{\tilde{C}_+}{\sqrt{c_2 + c_3 z_+} z_+} \log \left(\frac{\sqrt{c_2 + c_3 z_+} - \sqrt{c_2 + c_3 Z}}{\sqrt{c_2 + c_3 z_+} + \sqrt{c_2 + c_3 Z}} \frac{\sqrt{c_2 + c_3 z_+} + \sqrt{c_2}}{\sqrt{c_2 + c_3 z_+} - \sqrt{c_2}} \right) \\
&\quad + \frac{r_0}{b} \frac{r_0^2}{a^2} \left[\frac{r_{sc}^2 Z}{\sqrt{c_2} (Z-1)(z_- - 1)(z_+ - 1)} \right. \\
&\quad \left. - \frac{\sqrt{c_2} r_0^2}{(c_2 + c_3)(z_- - 1)(z_+ - 1)} \right. \\
&\quad \left. - \frac{\sqrt{c_2 + c_3 Z} r_0^2}{(c_2 + c_3)(Z-1)(z_- - 1)(z_+ - 1)} \right. \\
&\quad \left. + \frac{r_0^2 [2c_2(3 + z_-(z_+ - 2) - 2z_+) + c_3(7 - 5z_+ + z_-(3z_+ - 5))]}{2(c_2 + c_3)^{3/2} (z_- - 1)^2 (z_+ - 1)^2} \right. \\
&\quad \times \log \left(\frac{\sqrt{c_2 + c_3} + \sqrt{c_2 + c_3 Z}}{\sqrt{c_2 + c_3} - \sqrt{c_2 + c_3 Z}} \frac{\sqrt{c_2 + c_3} - \sqrt{c_2}}{\sqrt{c_2 + c_3} + \sqrt{c_2}} \right) \\
&\quad + \frac{r_0^2}{(z_- - 1)^2 z_- \sqrt{c_2 + c_3 z_-} (z_- - z_+)} \log \left(\frac{\sqrt{c_2 + c_3 z_-} - \sqrt{c_2 + c_3 Z}}{\sqrt{c_2 + c_3 z_-} + \sqrt{c_2 + c_3 Z}} \frac{\sqrt{c_2 + c_3 z_-} + \sqrt{c_2}}{\sqrt{c_2 + c_3 z_-} - \sqrt{c_2}} \right) \\
&\quad + \frac{r_0^2}{(z_+ - 1)^2 z_+ \sqrt{c_2 + c_3 z_+} (-z_- + z_+)} \log \left(\frac{\sqrt{c_2 + c_3 z_+} - \sqrt{c_2 + c_3 Z}}{\sqrt{c_2 + c_3 z_+} + \sqrt{c_2 + c_3 Z}} \frac{\sqrt{c_2 + c_3 z_+} + \sqrt{c_2}}{\sqrt{c_2 + c_3 z_+} - \sqrt{c_2}} \right) \\
&\quad - \frac{r_0^2 [-3 - z_-(z_+ - 2) + 2z_+]}{\sqrt{c_2} (z_- - 1)^2 (z_+ - 1)^2} \log \left(\frac{c_2(1 - Z)}{c_2 + c_3 Z} \right) \\
&\quad + \frac{r_0^2}{\sqrt{c_2} z_- z_+} \log \left(\frac{\sqrt{c_2 + c_3 Z} - \sqrt{c_2}}{\sqrt{c_2 + c_3 Z} + \sqrt{c_2}} \frac{c_2 + c_3 Z}{4c_3 Z} \right) \\
&\quad - \frac{r_0^2}{\sqrt{c_2} (z_- - 1)^2 z_- (z_- - z_+)} \log \left(\frac{c_2}{c_2 + c_3 Z} \frac{z_- - Z}{z_-} \right) \\
&\quad \left. - \frac{r_0^2}{\sqrt{c_2} (z_+ - 1)^2 z_+ (-z_- + z_+)} \log \left(\frac{c_2}{c_2 + c_3 Z} \frac{z_+ - Z}{z_+} \right) \right] . \tag{112}
\end{aligned}$$

The analytical expressions of I_D and I_R for the case of Kerr-Newman black holes are

similar to the formulas given above, but lengthy, and are omitted in this paper.

- [1] F. W. Dyson, A. S. Eddington, and C. Davidson, "IX. A determination of the deflection of light by the Sun's gravitational field, from observations made at the total eclipse of May 29, 1919", *Phil. Trans. R. Soc. A* 220, 291 (1920).
- [2] C. W. Misner, K. S. Thorne, and J. A. Wheeler, *Gravitation* (W. H. Freeman and Company, San Francisco, 1973).
- [3] S. Weinberg, *Gravitation and Cosmology: Principles and Applications of the General Theory of Relativity* (Wiley, New York, 1973).
- [4] J. B. Hartle, *Gravity: An Introduction to Einstein's General Relativity* (Addison-Wesley, 2003).
- [5] P. Schneider, J. Ehlers, and E. E. Falco, *Gravitational Lenses* (Springer-Verlag, New York, Berlin, Heidelberg, 1992).
- [6] S. Refsdal and J. Surdej, Gravitational lenses, *Rep. Prog. Phys.* 56, 117 (1994).
- [7] K. S. Virbhadra and G. F. R. Ellis, Schwarzschild black hole lensing, *Phys. Rev. D* 62, 084003 (2000).
- [8] S. Frittelli, T. P. Kling, and E. T. Newman, Spacetime perspective of Schwarzschild lensing, *Phys. Rev. D* 61, 064021 (2000).
- [9] V. Bozza, S. Capozziello, G. Iovane, and G. Scarpetta, Strong field limit of black hole gravitational lensing, *Gen. Relativ. Gravit.* 33, 1535 (2001).
- [10] V. Bozza, Gravitational lensing in the strong field limit, *Phys. Rev. D* 66, 103001 (2002).
- [11] V. Bozza, Quasiequatorial gravitational lensing by spinning black holes in the strong field limit, *Phys. Rev. D* 67, 103006 (2003).
- [12] E. F. Eiroa, G. E. Romero, and D. F. Torres, Reissner-Nordstrom black hole lensing, *Phys. Rev. D* 66, 024010 (2002).
- [13] V. Bozza and G. Scarpetta, Strong deflection limit of black hole gravitational lensing with arbitrary source distances, *Phys. Rev. D* 76, 083008(2007).
- [14] S. V. Iyer and A. O. Petters, Light's bending angle due to black holes: From the photon sphere to infinity, *Gen. Relativ. Gravit.* 39, 1563 (2007).
- [15] N. Tsukamoto, Deflection angle in the strong deflection limit in a general asymptotically flat, static, spherically symmetric space-time, *Phys. Rev. D* 95, 064035 (2017).

- [16] N. Tsukamoto and Y. Gong, Retrolensing by a charged black hole, *Phys. Rev. D* 95, 064034 (2017).
- [17] K. Akiyama et al., Event horizon telescope collaboration, First M87 event horizon telescope results. I. The shadow of the supermassive black hole, *Astrophys. J.* 875, L1 (2019).
- [18] K. Akiyama et al., Event horizon telescope collaboration, First M87 event horizon telescope results. V. Physical origin of the asymmetric ring, *Astrophys. J.* 875, L5 (2019).
- [19] K. Akiyama et al. Event horizon telescope collaboration, First M87 event horizon telescope results. VI. The shadow and mass of the central black hole, *Astrophys. J.* 875, L6 (2019).
- [20] T. Hsieh, D.-S. Lee, and C.-Y. Lin, Strong gravitational lensing by Kerr and Kerr-Newman black holes, *Phys. Rev. D.* 103, 104063 (2021).
- [21] S. V. Iyer and E. C. Hansen, Light's bending angle in the equatorial plane of a Kerr black hole, *Phys. Rev. D* 80, 124023 (2009).
- [22] Y.-W. Hsiao, D.-S. Lee, and C.-Y. Lin, Equatorial light bending around Kerr-Newman black holes, *Phys. Rev. D.* 101, 064070 (2020).
- [23] I. Z. Stefanov, S. S. Yazadjiev, and G. G. Gyulchev, Connection between Black-Hole Quasi-normal Modes and Lensing in the Strong Deflection Limit, *Phys. Rev. Lett.* 104, 251103 (2010).
- [24] B. Raffaelli, Strong gravitational lensing and black hole quasinormal modes: towards a semi-classical unified description, *Gen. Relativ. Gravit.* 48, 16 (2016).
- [25] V. Bozza and L. Mancini, Time delay in black hole gravitational lensing as a distance estimator, *Gen. Relativ. Gravit.* 36, 435 (2004).
- [26] C. R. Keeton and A. O. Petters, Formalism for testing theories of gravity using lensing by compact objects: Static, spherically symmetric case, *Phys. Rev. D.* 72, 104006 (2005).
- [27] C. R. Keeton and A. O. Petters, Formalism for testing theories of gravity using lensing by compact objects. II. Probing post-post-Newtonian metrics, *Phys. Rev. D.* 73, 044024 (2006).
- [28] K. S. Virbhadra and C. R. Keeton, Time delay and magnification centroid due to gravitational lensing by black holes and naked singularities, *Phys. Rev. D* 77, 124014 (2008).
- [29] K. S. Virbhadra, Relativistic images of Schwarzschild black hole lensing, *Phys. Rev. D* 79, 083004 (2008).
- [30] X. Lu, F.-W. Yang and Y. Xie, Strong gravitational field time delay for photons coupled to Weyl tensor in a Schwarzschild black hole, *Eur. Phys. J. C* 76, 357 (2016).

- [31] T. Adamo and E. T. Newman, The Kerr-Newman metric: A review arXiv:1410.6626.
- [32] C.-Y. Liu, D.-S. Lee, and C.-Y. Lin, Geodesic motion of neutral particles around a Kerr-Newman black hole, *Class. Quantum Grav.* 34, 235008 (2017).
- [33] C. Jiang and W. Lin, Post-Newtonian light propagation in Kerr-Newman spacetime, *Phys. Rev. D* 97, 024045 (2018).
- [34] G. V. Kraniotis, Gravitational lensing and frame dragging of light in the Kerr-Newman and the Kerr-Newman (anti) de Sitter black hole spacetimes, *Gen. Relativ. Gravit.* 46, 1818 (2014).
- [35] A. Ghez, et al., High proper-motion stars in the vicinity of Sagittarius A*: Evidence for a supermassive black hole at the center of our galaxy, *Astrophysical Journal.* 509, 678 (1998).
- [36] R. Schodel, et al. A star in a 15.2-year orbit around the black hole at the centre of the Milky Way, *Nature.* 419, 694 (2002).
- [37] D. Richstone et al., Supermassive black holes and the evolution of galaxies, *Nature (London)* 14, 395 (1998).
- [38] G. Fragione and A. Loeb, An upper limit on the spin of SgrA* based on stellar orbits in its vicinity, *The Astrophysical Journal Letters,* 901, L32 (2020).
- [39] F. Tamburini, B. Thide and M. D. Valle, Measurement of the spin of the M87 black hole from its observed twisted light, *Monthly Notices of the Royal Astronomical Society* 492, L22 (2020).
- [40] J. S. Ulvestad, Goals of the ARISE Space VLBI Mission, *New Astron. Rev.* 43, 531 (1999).
- [41] M. D. Johnson, et al. Universal interferometric signatures of a black hole's photon ring, *Sci. Adv.* 6, eaaz1310 (2020).
- [42] S. E. Gralla and A. Lupsasca, Null geodesics of the Kerr exterior, *Phys. Rev. D* 101, 044032 (2020).
- [43] S. E. Gralla and A. Lupsasca, Lensing by Kerr black holes, *Phys. Rev. D* 101, 044031 (2020).